Article

Homogenous UV/Periodate Process for the Treatment of Acid Orange 10 Polluted Water

Maroua Nessaibia [1], Houria Ghodbane [2], Hana Ferkous [3,4], Slimane Merouani [5], Manawwer Alam [6], Marco Balsamo [7], Yacine Benguerba [8] and Alessandro Erto [9,*]

[1] Laboratory Sciences and Technical Water and Environment, Faculty of Science and Technology, Mohamed Cherif Messaadia University, Souk-Ahras 41000, Algeria
[2] Laboratory of Physics of Matter and Radiation, Mohamed Cherif Messadia-Souk Ahras University, Souk Ahras 41000, Algeria
[3] Laboratory of Mechanical Engineering and Materials, Faculty of Technology, University 20 August 1955 of Skikda, Skikda 21000, Algeria
[4] Department of Technology, University 20 August 1955 of Skikda, Skikda 21000, Algeria
[5] Department of Chemical Engineering, Faculty of Process Engineering, University Constantine 3-Salah Boubnider, Constantine 25000, Algeria
[6] Department of Chemistry, College of Science, King Saud University, Riyadh 11451, Saudi Arabia
[7] Department of Chemical Sciences, University of Naples Federico II, Complesso Universitario di Monte Sant'Angelo, 80126 Napoli, Italy
[8] Laboratory of Biopharmaceuticals and Pharmaceutical Technology (LBPT), Ferhat Abbas Setif 1 University, Setif 19000, Algeria
[9] Department of Chemical, Materials and Production Engineering, University of Naples Federico II, P.le Tecchio, 80, 80125 Napoli, Italy
* Correspondence: aleserto@unina.it

Abstract: The photoactivated periodate (UV/IO_4^-) process is used to investigate the degradation of acid orange 10 (AO10) dye. The photodecomposition of periodate ions produces highly reactive radicals (i.e., $^\bullet OH$, $IO_3^\bullet$, and $IO_4^\bullet$) that accelerate dye degradation. Increasing the initial concentration of periodate to 3 mM enhances the dye removal rate, but over 3 mM periodate, the degradation rate slows down. On the contrary, increasing initial dye concentrations reduces the degradation performance. pH is the most critical factor in AO10 breakdown. Salts slow down the degradation of the dye. However, UV/IO_4^- is more efficient in distilled water than natural water. Even at low concentrations, surfactants may affect the dye's decomposition rate. The addition of sucrose reduced the breakdown of AO10. Although tertbutanol is a very effective $^\bullet OH$ radical scavenger, it does not affect the dye breakdown even at the highest concentrations. Accordingly, the AO10 degradation is a non-$^\bullet OH$ pathway route. According to retrieved data, the photoactivated periodate method eliminated 56.5 and 60.5% of the initial COD after 60 and 120 min of treatment time; therefore, it can be concluded that the UV/IO_4^- system may treat effluents, especially those containing textile dyes.

Keywords: acid orange 10; wastewater; advanced oxidation process; periodate; ultraviolet irradiation; degradation kinetics

1. Introduction

The increasing number of pollutants (organic and inorganic) in aquatic ecosystems (e.g., ground and surface waters) is mainly caused by wastewater released by domestic and industrial activities. Due to more severe environmental regulations, there is a need to develop eco-sustainable cleansing technologies characterized by high decontamination efficiency and low costs. In particular, eliminating toxic and non-biodegradable organic dyes from liquid effluents represents a significant technological challenge since these molecules are difficult to break down due to their complex aromatic structure and persistent characteristics [1]. The bio-treatment of dye pollution is inefficient because of its resistance

to aerobic treatment. During anaerobic dye processing, carcinogenic aromatic amines may also be formed, thus creating undesired secondary pollutants [2–8]. Adsorption of dyes on different sorbents (such as activated carbons) have been considered previously; however, it is a non-destructive route that merely transfers the pollutant molecules to another medium, and a proper regeneration treatment is required to continuously apply the sorbent and recover the dye in concentrated form. At the same time, large quantities and high sludge doses make chemical approaches for eliminating color pollution expensive options. The current scenario necessitates new and improved methods for wastewater treatment because of the ineffectiveness of some of the technologies discussed above [1]. Many scientists and engineers have suggested new advanced oxidation processes (AOPs) to degrade organic dyes while minimizing secondary pollution under normal operating conditions.
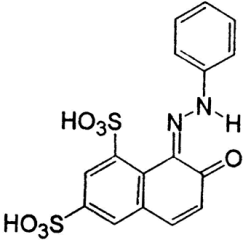
Recently, periodate (IO_4^-)-based AOPs have shown to be of great interest in the field of water treatment [9]. Periodate may be activated by H_2O_2 [10], activated carbon [11], iodine-doped granular activated carbon [12], cobalt/carbon nanotubes (Co/CNTs) [13], UV light [14], and other techniques [9]. Periodate (IO_4^-) photoactivation decomposes various persistent organic contaminants and reduces chemical oxygen demand in industrial wastewater. The photo-irradiation of periodate (light with $\lambda < 400$ nm) may generate multiple reactive radicals and non-radical species, including $^\bullet OH$, $IO_3^\bullet$, $IO_4^\bullet$, H_2O_2, $O(^3P)$, O_3 and IO_3^-, which work together to speed up the degradation process when compared to UV, UV/H_2O_2 and other UV-based AOPs. The UV/IO_4^- reaction mechanism has previously been studied in deionized water using various techniques across a wide pH range [15–19]. Periodate often undergoes the following photolytic reactions in the pH range from 2 to 8 [20–27]:

$$IO_4^-(^{IVII}) + h\nu \rightarrow IO_3^\bullet(^{IVI}) + O^{\bullet -} \tag{1}$$

$$IO_4^- + h\nu \rightarrow IO_3^- + O(^3P) \tag{2}$$

$$O^{\bullet -} + H^+ \rightarrow {}^\bullet OH \tag{3}$$

$$O(^3P) + O_2 \rightarrow O_3 \tag{4}$$

$$IO_4^- + IO_3^\bullet \rightarrow IO_4^\bullet + IO_3^- \tag{5}$$

$${}^\bullet OH + IO_4^- \rightarrow OH^- + IO_4^\bullet \tag{6}$$

$$IO_3^- + {}^\bullet OH \rightarrow HIO_4^- \tag{7}$$

$$IO_3^- + {}^\bullet OH \rightarrow IO_3^\bullet + OH^- \tag{8}$$

$${}^\bullet OH + {}^\bullet OH \rightarrow H_2O_2 \tag{9}$$

$$O(^3P) + O(^3P) \rightarrow O_2 \tag{10}$$

$$2IO_3^\bullet \rightarrow I_2O_6 \tag{11}$$

$$I_2O_6 + H_2O \rightarrow IO_4^- + IO_3^- + 2H^+ \tag{12}$$

$$2IO_4^\bullet \rightarrow I_2O_8 \tag{13}$$

$$I_2O_8 + H_2O \rightarrow IO_3^- + IO_4^- + 2H^+ + O_2 \tag{14}$$
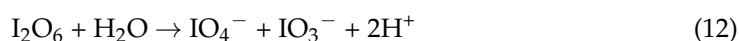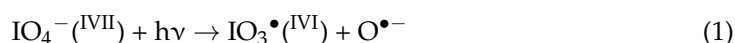
The radicals and reactive species generated by periodate photolysis make the oxidation of persistent organic molecules more feasible [28]. Figure 1 reports the radicals derived from the generation, transformation, and interconversion pathways proposed in the literature [29]. The literature has reported that the decomposition of IO_3^- results in lower quantum yields than IO_4^-; therefore, periodate may lead to greater reaction efficiency [30]. There is currently no environmental legislation on releasing iodine compounds in water, where I_2 and I^- may be the most warned. Iodine can be recuperated by ion exchange, while periodate can be regenerated by electrochemical means [31]. Ilin and Nersesyan [32] found that $IO_3^\bullet$ had no mutagenic impact on the Salmonella TA98/TA100 strains. The ion exchange mechanism converts iodine compounds into periodate species, and this

iodine may be recovered before discharge. There is substantial research on photoactivated periodate in acidic solutions, but little is known about its use in alkaline solutions.

Figure 1. Schematic UV/IO_4^- process radical and reactive species production, transformation, and interconversion. Reprinted/adapted with permission from Ref. [29]. 2023, Elsevier.

This paper deals with the application of UV/IO_4^- process for degrading one of the most persistent and toxic azo dyes, acid orange 10 (AO10), which is widely used in textile and many manufacturing processes. Even though several AOPs (e.g., Sonolysis, photolysis, etc.) were applied for the degradation of this chemical, there are no studies about the application of UV/periodate system for abating this dangerous substance. Thus, to get a more comprehensive knowledge on the effect of operating conditions on AO10 removal performances, a deep experimental analysis was performed. The impacts of key operational conditions, the presence of other components in the treated water medium (e.g., inorganic ions, sucrose, and surfactants) and natural water matrices were all elucidated.

2. Materials and Methods

2.1. Chemical Reagents

Acid orange 10 (1-phenylazo-2-naphthol-6, 8-disulfonic acid, disodium salt AO10; CI number: 16230; azo chemical class: $C_{16}H_{10}N_2Na_2O_7S_2$); supplied by Sigma-Aldrich, St. Louis, MO, USA) was used in this study as a representative dye for the investigation of its degradation by UV/IO_4^- treatment. Table 1 reports the AO10's molecular structure and some other specifications. Sodium hydroxide or sulfuric acid (Sigma-Aldrich, St. Louis, MO, USA) were employed to adjust the pH of the solution. Sodium periodate, sodium sulfate, and potassium bromide were purchased from Acros Organics. Hexadecyltrimethylammonium bromide (CTAB), Tween 80 and Triton X100, which were used to test the effect of surfactants on AO10 degradation, were supplied by Sigma-Aldrich. Periodate solutions were prepared in distilled water. All purchased products had the purest grade available (>99%).

Table 1. The characteristics of acid orange 10 (AO10) dye.

Structure	
Formula:	$C_{16}H_{10}N_2Na_2O_7S_2$
M_W = 452.36 g/mol;	λ_{max} = 477 nm

2.2. Photoreactor

A batch photoreactor with a capacity of 500 mL was adopted for the AO10 degradation experiments. A thermocouple was inserted into the reaction medium to measure the temperature of the solution. The temperature within the reactor was controlled at 20 ± 1 °C by circulating water in a cooling jacket surrounding the reactor. A 25 W low-pressure mercury lamp (intensity: 15 mW/cm^2) with a maximum emitting wavelength of 254 nm was adopted to deliver UV-C irradiation for the experiment. A quartz tube housed the UV-C lame (Figure 2). This was later positioned at the center of the cell, 2 cm above the bottom.
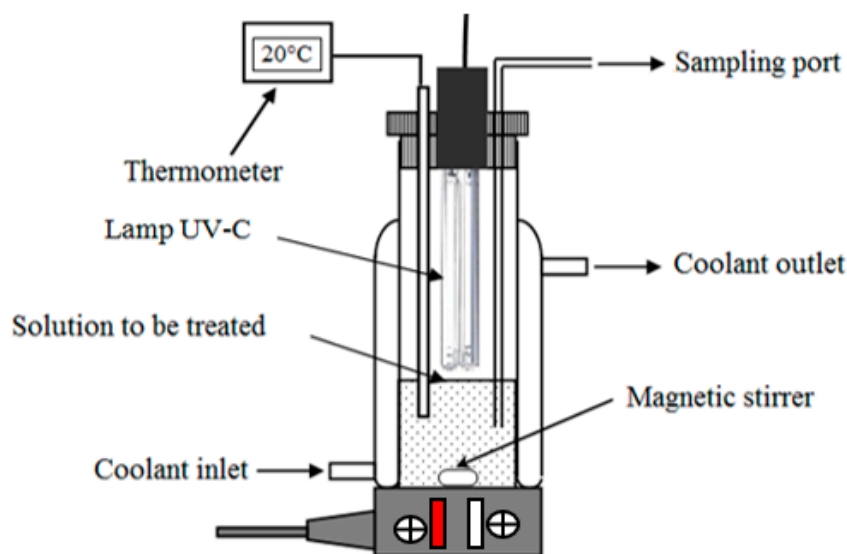
Figure 2. AO10 degradation photoreactor.

2.3. Analytical Methodologies and Experimental Procedures for AO10 Degradation Tests

The photolytic degradation of AO10 was carried out in a cylindrical water-jacketed glass reactor with a constant solution volume of 200 mL. Circulating water was used to maintain a constant temperature of 20 °C for the solution. During the whole irradiation process, 300 rpm of magnetically constant stirring was utilized. Regular dye absorbance measurements were taken during AO10 degradation using a spectroFlex 6600 UV-VIS (photoLab® 6600, Cincinnati, OH, USA) spectrophotometer at 477 nm to determine the dye concentration (a calibration curve was established prior, with non-recorded impact of pH 2–11 on λ_{max}). All experiments were performed in triplicate, and the average results of each test were recorded and reported. Error bars incorporated in the relevant graphs show the highest deviation of the mean.

Using potassium dichromate ($K_2Cr_2O_7$) as an oxidant in an acidic solution (H_2SO_4), the method proposed by Thomas and Mazas [33] was adopted for the determination of chemical oxygen demand (COD). The method utilized Hg^{2+} complexing agent and an Ag_2SO_4 catalyst. In COD analyzer, samples were heated to 150 °C for 2 h. The excess of potassium dichromate was detected using a UV-visible spectrophotometer. The COD value was calculated by comparing the initial dichromate concentration to the amount not consumed during chemical oxidation.

3. Results and Discussion

3.1. Photo-Decomposition of Periodate Ions

Figure 3 shows how UV irradiation of IO_4^- aqueous solution (neutral pH, without AO10) affects the UV absorption spectra (especially λ_{max} = 221 nm of periodate). As the UV light was delivered to the solution, the concentration of the periodate ion dropped over the first 10 min to 0.5% of its initial concentration (absorbance). These outcomes confirm the rapid photodecomposition (at 254 nm) of periodate ions into reactive species and by-products. The same observation was previously reported by other research, working at different operating conditions [21,34].
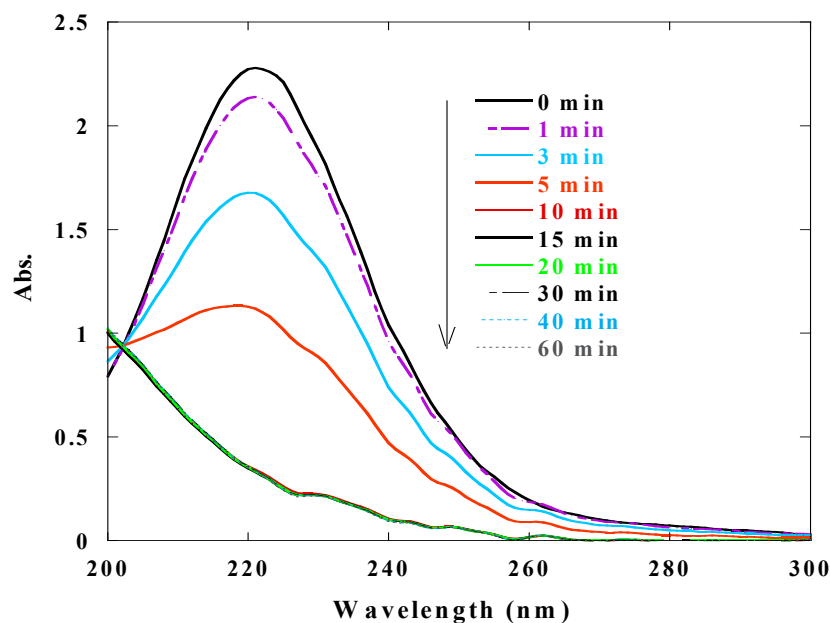
Figure 3. Absorption spectra of UV-irradiated IO_4^- aqueous solution ($[IO_4^-]$ = 0.5 mM, 20 ± 1 °C, irradiation intensity: 15 mW/cm^2).

### 3.2. Effect of Periodate Concentration

Many runs were carried out to investigate the degradation of AO10 (50 mg/L) under the sole UV exposure (data not shown). Roughly 300 min of treatment time is required to completely degrade the dye under the investigated conditions (i.e., 50 mg/L). Extended treatment times are undoubtedly detrimental in terms of reduced UV lamp lifetime. Therefore, the presence of photoactivated periodate ions was contemplated to compensate for this inconvenience and gain better degradation results. Figure 4 shows the initial degradation rate of AO10 (mg/L min) calculated over the first 5 min, both under sole UV irradiation and in the presence of periodate at different initial concentrations, and natural pH (5.4).
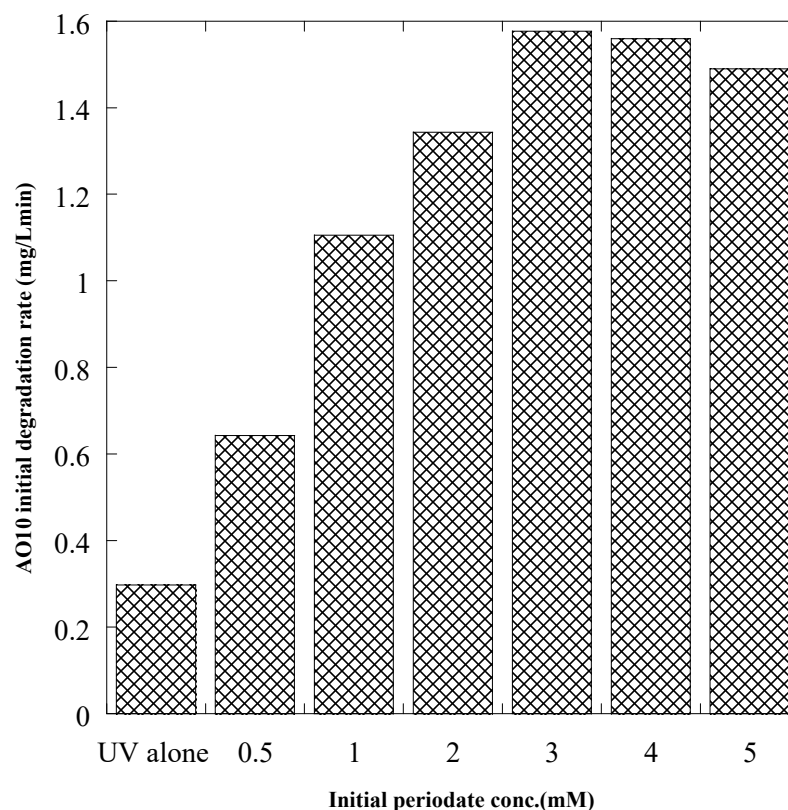
Figure 4. Effect of the $[IO_4^-]$ on the initial degradation rate of AO10 ($[AO10]_0 = 50$ mg/L, 20 ± 1 °C, initial pH 5.4, irradiation intensity: 15 mW/cm^2).

Overall, the results show the effectiveness of adding periodate in the liquid medium for accelerating the initial degradation rate of the dye pollutant. The initial degradation rate of AO10 was about 0.3 mg/L min when adopting only UV irradiation; this value was multiplied by 3.7 and 5.5-fold in the presence of IO_4^- at 1 and 3 mM, respectively. However, raising IO_4^- concentration above 3 mM had a limited impact on the dye degradation rate because of the scavenger role played by periodate (when it is in excess) toward free radicals [23]. It is important to stress here that periodate alone (without UV) did not affect the dye removal for up to 60 min. Therefore, the obtained synergic effect resulted mainly from the photoactivation of IO_4^-, which yields reactive contributions (as stated in the introduction).

Figure 5 elucidates the whole C/C_0-concentration evolutions (for 150 min), in the absence and presence of periodate (same dosages of Figure 4). An increase in AO10's removal (%) was observed due to the IO_4^- presence. After 90 min of UV exposure, the removal efficiency rose from 47.15% to 81.50, 95, 98.10 and 99.20% when $[IO_4^-]_0$ was used at 0.5, 1, 2 and 3 mM. High periodate load (but <3 mM) may boost IO_4^--incident light absorption and generate more $^\bullet OH$ and $IO_3^\bullet$ that react with AO10, resulting in an increase in the degradation rate. It is interesting to note that the degradation process occurs slowly at low IO_4^- concentrations but speeds up when the IO_4^- concentration rises since IO_4^- could produce byproducts such as $IO_3^\bullet$ and $^\bullet OH$ via Reaction (6). However, Reaction (11), which has a high-rate constant of 7.6×10^8 M^{-1} s^{-1} [35], is a significant parasitic reaction that slows down the degradation of the dye at heavily loaded periodate (5 mM). Hamdaoui and Merouani [22] and Ghordbane and Hamdaoui [21] reported the same detrimental effect of high IO_4^- concentrations on the sono-degradation and photo-destruction of many dyes.
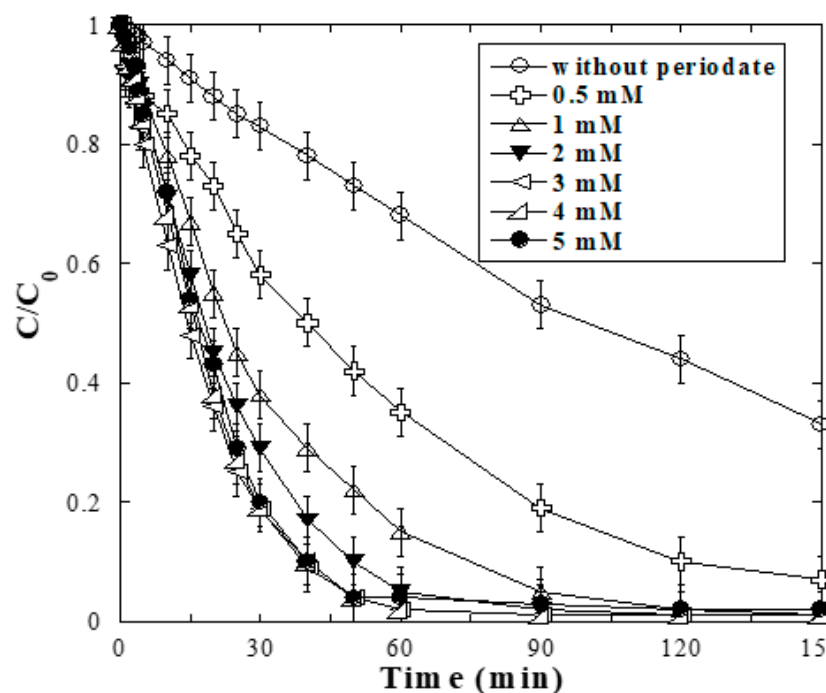
Figure 5. AO10 degradation kinetics versus $[IO_4^-]_0$ ($[AO10]_0 = 50$ mg/L, Temp. 20 ± 1 °C, initial pH 5.4, irradiation intensity: 15 mW/cm^2).

3.3. Effect of Initial pH

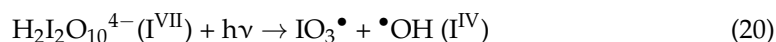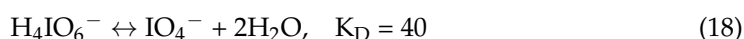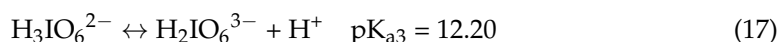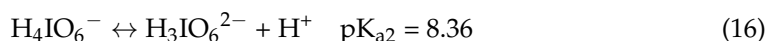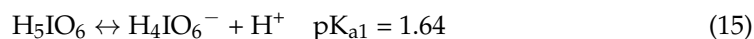Bendjama et al. [23] showed that acidic solutions (pH 2–4) improved the breakdown efficiency of chlorazol black (CB) in saline water. Lee and Yoon [24] found that the pH between 1.5 and 10 had no significant influence on the degradation of the reactive dye black 5. Moreover, a pH of 7.6 was the best operating condition for eliminating triethanolamine and AB25 [21–27]. Therefore, the effect of pH on the effectiveness of UV/periodate treatment is not well established, probably due to the more complicated reaction mechanism in the presence of organic solutes. This controversy may also be related to different operating conditions being adopted (irradiation wavelength, reactant doses, etc.), in addition to different chemical structures/nature of the pollutants investigated in the cited work.

In the present work, a pH range of $1-10$ was selected to examine the effect of this parameter on UV/IO_4^- treatment for the remediation of AO10 ($C_0 = 50$ mg/L) by adopting an IO_4^- concentration of 3.0 mM. Results reported in Figure 6 indicate that the degradation rate increased with pH increase from 1 to 5.4 and then decreased afterward. The lowest degradation rate was observed at pH 10. At pH < 8, IO_4^- species dominated, while the dimerized form, $H_2I_2O_{10}^{4-}$, was the dominant species above pH 8. Under acidic conditions (pH 1–3), the reduction of the initial degradation rate of AO10 by UV/IO_4^- could be linked to the presence of H^+ and SO_4^{2-} ions arising from the addition of sulphuric acid [21]. These anions may act as radicals' scavenger, thereby altering the degradation process. At pH 5.4, the concentration of these species is lower, which increased the probability of radical quenching by the dye molecules instead of the mineral anions. It should be noted that acid dyes are usually used for dyeing wool and nylon. Our process is typically carried out in an acid medium because it is necessary to produce positively charged fibers by protonation. This way, the dye is mainly fixed to the fiber by electrostatic forces.
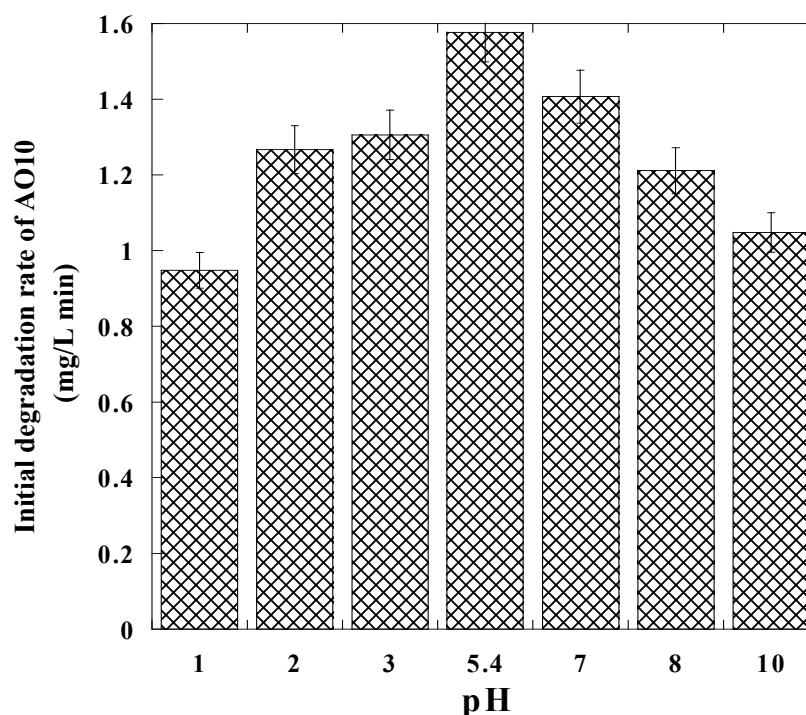
Figure 6. Effect of the initial pH on the AO10 degradation rate ($[AO10]_0$ = 50 mg/L, 20 ± 1 °C, $[IO_4^-]$ = 3 mM, irradiation intensity: 15 mW/cm^2).

Periodate ions in water can be present in various forms, i.e., IO_4^-, $H_2IO_6^{3-}$, $H_3IO_6^{2-}$, $H_4IO_6^-$, H_5IO_6 and $H_2I_2O_{10}^{4-}$, and their molar fraction depends on the pH and the concentration of IO_4^- [36]. The speciation diagram of these species may be described by the following periodate hydrolysis/dimerization reactions:

$$H_5IO_6 \leftrightarrow H_4IO_6^- + H^+ \quad pK_{a1} = 1.64 \tag{15}$$

$$H_4IO_6^- \leftrightarrow H_3IO_6^{2-} + H^+ \quad pK_{a2} = 8.36 \tag{16}$$

$$H_3IO_6^{2-} \leftrightarrow H_2IO_6^{3-} + H^+ \quad pK_{a3} = 12.20 \tag{17}$$

$$H_4IO_6^- \leftrightarrow IO_4^- + 2H_2O, \quad K_D = 40 \tag{18}$$

$$2H_3IO_6^{2-} \leftrightarrow H_2I_2O_{10}^{4-} + 2H_2O \quad K_X = 141 \ M^{-1} \tag{19}$$

$$H_2I_2O_{10}^{4-} (I^{VII}) + h\nu \rightarrow IO_3^\bullet + {}^\bullet OH \ (I^{IV}) \tag{20}$$

At pH levels greater than 8, $H_2I_2O_{10}^{4-}$ species predominate, whereas IO_4^- tetrahedral anion species predominate between pH 1 and 8. In particular, $H_2I_2O_{10}^{4-}$ can be photodegraded into the radicals ${}^\bullet OH$ and $IO_3^\bullet$, as suggested by [24,37]. In our case, the breakdown of AO10 may selectively convert $IO_3^\bullet$ to IO_3^-, according to the following general equation:

$$IO_3^\bullet(I^{VI}) + \text{contaminant molecule} \rightarrow IO_3^- \ (I^V) + \text{oxidized product} \tag{21}$$

When AO10 is exposed to UV light for 20 min at a pH of 5.4 (control pH), the process performance is best. This is because acidic conditions create intermediate iodine radicals such as $IO_3^\bullet$ and $IO_4^\bullet$, which play a crucial role alongside ${}^\bullet OH$ in the photo-assisted elimination of chemical compounds [23]. However, for the examined system, AO10 degradation may occur throughout a broad pH range (up to 10), revealing the advantage of the UV/periodate process compared to many other AOPs (e.g., Fenton, UV/H_2O_2), when a high pH level may restrict the effectiveness of their applications.
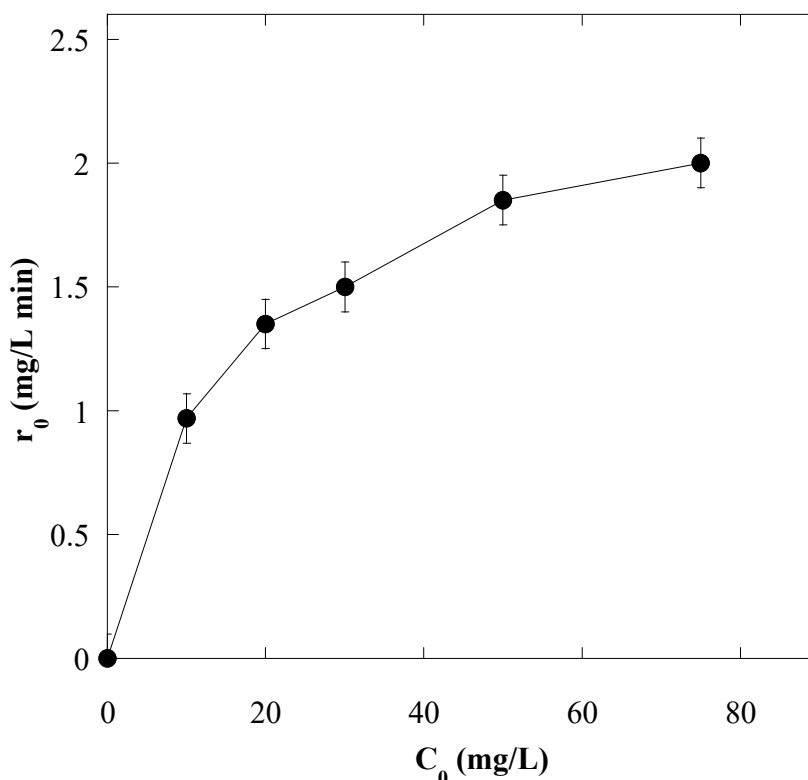
3.4. Effect of Initial Dye Concentration

To broaden the research validity and applications, the breakdown efficiency of AO10 in the presence of 3 mM periodate was investigated for a wide range of initial concentrations (10, 20, 30, 50 and 75 mg/L). The results are depicted in Figure 7. The degradation efficiency dropped monotonically with C_0 increase; the removal (after only 10 min) being 99.50% for $C_0 = 10$ mg/L against 34.70% for $C_0 = 75$ mg/L. This may be due to a competition phenomenon between the dye molecules and degradation byproducts generate a reaction with free radicals [21]. In fact, a considerable number and number of intermediates are produced when AO10 concentrations are increased. In addition, high color intensity could block the passage of light into the bulk solution (which improves the solution's internal optical density), thus reducing the yield of periodate photolysis (i.e., to general radicals) [38].
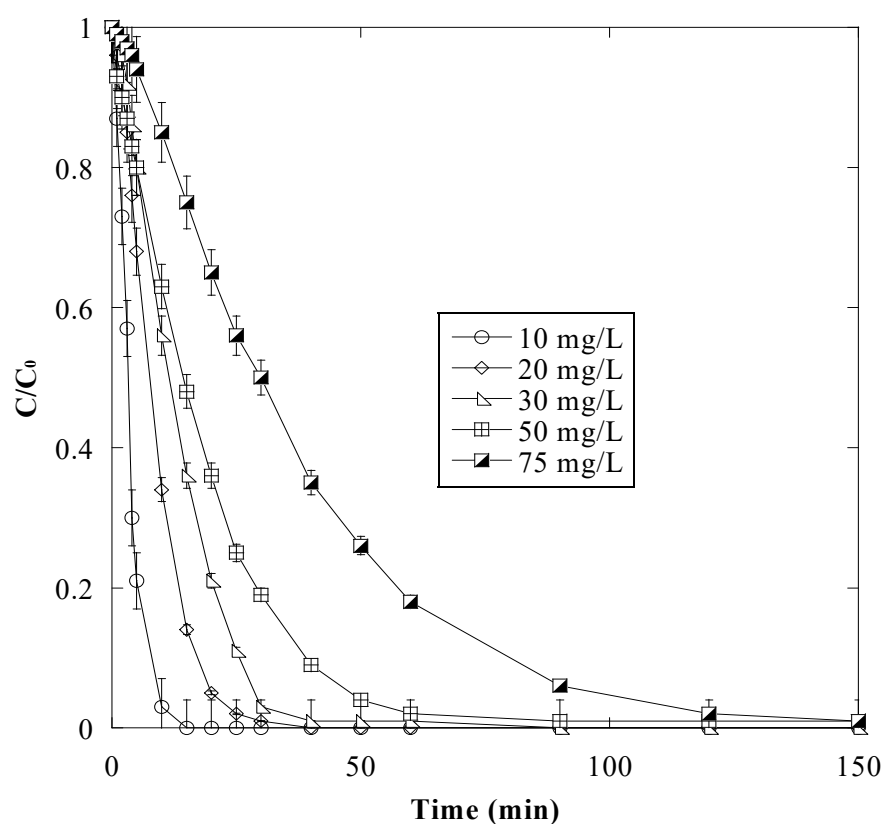
Figure 7. Effect of initial AO10 concentration on its degradation ($[A010]_0 = 10–75$ mg/L, 20 ± 1 °C, $[IO_4^-] = 3$ mM, initial pH 5.4, irradiation intensity: 15 mW/cm^2).

The plot of initial degradation rate (r_0, calculated from Figure 7) vs. initial AO10 concentration, C_0, (Figure 8) clearly shows a non-linear relation between r_0 and C_0, which excludes the validity of first order kinetic law for the degradation of AO10. In fact, if the reaction rate would obey this law, r_0 vs. C_0 should follow the linear relationship $r_0 = k.C_0$ [39]. Therefore, all the AO10 degradation patterns (conducted in this project) could be discussed based on the removal of kinetics profiles (C/C_0 vs. time), in addition to the initial degradation rate (r_0, in mg/(L min)) rather than the use of the pseudo-first-order constant (k, expressed in s^{-1}). This means that the overall degradation rate could be controlled by both the pollutant concentration as well as the free radical concentration. Many AOPs researchers have already pointed this out in many publications [23,34,40].

Figure 8. Initial AO10 degradation rate (r_0) vs. its initial concentration C_0, under the same conditions of Figure 8.

3.5. Effect of Inorganic Anions

Three common anions (Cl^-, SO_4^{2-}, Br^-) were used to investigate the impact of water constitutes on the degradation of AO10 by UV/IO_4^-. Figure 9 depicts the degradation of AO10 under various conditions as the concentrations of the three anions rose from 0 to 0.1, 0.5, 1, 3, and 5 g/L. As a general comment, all the anions showed a detrimental effect on AO10 degradation, which is generally marked at increasing salt concentration. Among the tested ionic species, chloride produces a minor reduction of the degradation efficiency of AO10, while it is significantly reduced in the presence of SO_4^{2-}. The removal of AO10 was 58.97, 52.42, 50.45, 49.78 and 48.34%, at Cl^- concentrations of 0.1, 0.5, 1, 3 and 5 g/L, respectively, whereas the removal rate was 64% in absence of Cl^-. The inhibited degradation of AO10 was related to the ability of Cl^- (at high concentration) to react with $^\bullet OH$ (scavenging role) [41]. Chloride ions also react with iodine radicals to a certain extent [41]. These reactions result in the production of a radical less reactive than $^\bullet OH$ and iodine radicals (i.e., $HOCl^{\bullet -}$) [28]. According to Bendjama and colleagues [23], chloride did not affect the interaction of CB with iodine radicals generated by UV light at seawater concentrations (500 mg/L). Contrary to chlorine ions, sulfate did not alter significantly the degradation of the dye, even in the presence of high SO_4^{2-} dosage, which is probably because sulfate ions are generally eco-friendly to reactive oxidants in most AOPs [42]. The most inhibiting impact is that retrieved in the case of bromide ions. AO10 removal fell from 64.08% without KBr to 24.60, 27.35, 26.56, 23.21 and 23.13%, respectively, with KBr addition at 0.1, 0.5, 1, 3, and 5 g/L, confirming the effective inhibition in the degradation of dye (Figure 9). A similar generated trend (to that of bromide ions) was reported by Chadi et al. [43], which treated Toluidine Blue dye by H_2O_2/IO_4^- process (periodate is activated by H_2O_2 in this process).
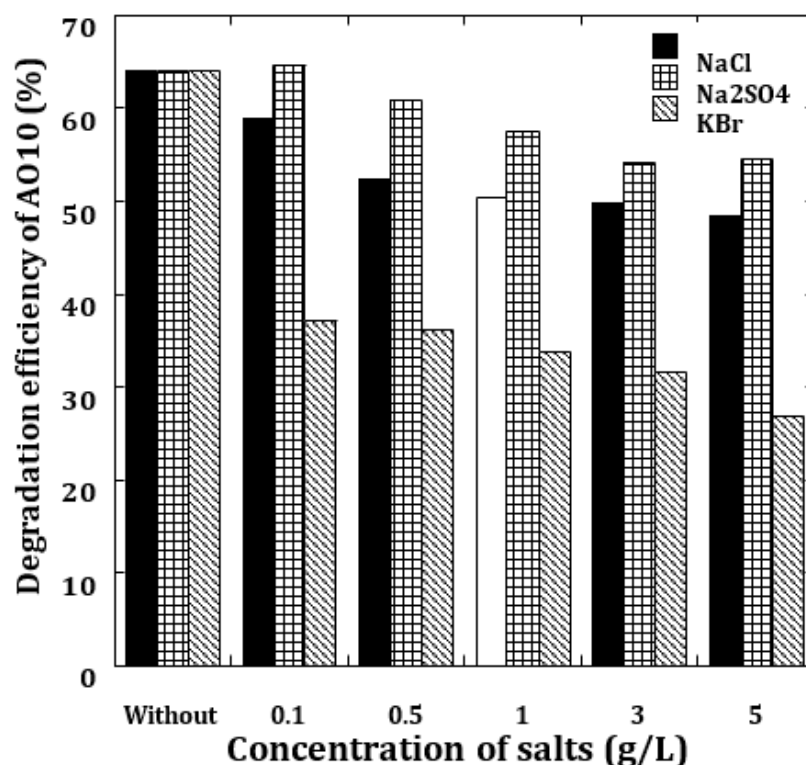
Figure 9. Effect of different salts on the degradation efficiency of AO10 ($[A010]_0 = 50$ mg/L, 20 ± 1 °C, $[IO_4^-] = 3$ mM, irradiation intensity: 15 mW/cm^2).

3.6. Effect of Water Matrix Components

To test the applicability of the UV/IO_4^- process for the degradation of AO10 in realistic water conditions, experiments were performed in natural mineral water and seawater having the following characteristics:

- Natural mineral water: pH 7.2, $Ca^{2+} = 81$ mg L^{-1}, $Mg^{2+} = 24$ mgL^{-1}, $Na^+ = 15.8$ mg L^{-1}, $Cl^- = 72$ mg L^{-1}, $SO_4^{2-} = 53$ mg L^{-1}, $HCO_3^- = 265$ mg L^{-1}.
- Seawater: pH 7.6, $Ca^{2+} = 416$ mg L^{-1}, $Mg^{2+} = 1295$ mg L^{-1}, $Na^+ = 11{,}600$ mg L^{-1}, $Cl^- = 21{,}400$ mgL^{-1}, $SO_4^{2-} = 3060$ mg L^{-1}, $Br^- = 66$ mg L^{-1}, $Sr^{2+} = 27$ mg L^{-1}, $B^{3+} = 13$ mg L^{-1}, $F^- = 1$ mg L^{-1}.

Figure 10 shows the results of AO10 degradation performed in real water matrices and compared to the outcomes obtained in distilled water. As expected, the experimental results show a reduction in the removal efficiency of AO10 in both natural mineral water and seawater. Nevertheless, after 150 min of treatment time, almost 80% of the dye's abatement efficiency could still be inferred for both real water matrices. The presence of Cl^- and SO_4^{2-} ions have a detrimental effect by acting as radical scavengers [43–45]. Moreover, salts (in seawater and natural mineral water) function as light screens and reduce the photon receiving efficiency (light attenuation effect) and, consequently, the degradation rate of the target pollutant. Bendjama et al. [23] recorded about 20% decrease in the efficiency of chlorazol black removal in seawater (against deionized water). They attributed this difference mainly to the physical effect of salts load on the dispersion of light, i.e., light screening filter.
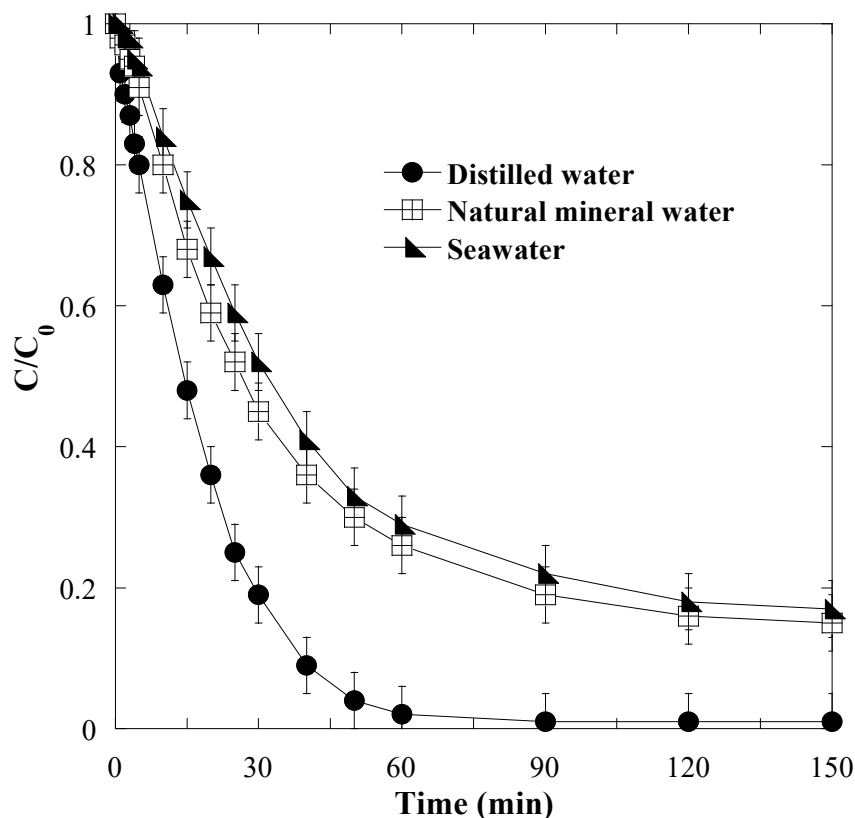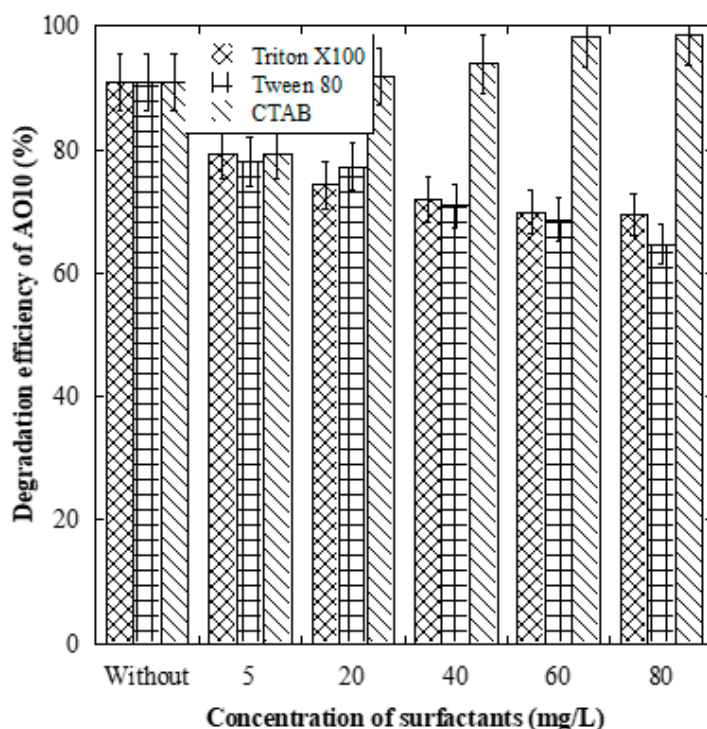
Figure 10. Effect of water matrix on the A010 degradation ([AO10]$_0$ = 50 mg/L, 20 $\pm$ 1 °C, [IO$_4^-$] = 3 mM, irradiation intensity: 15 mW/cm^2).

3.7. Effect of Surfactants on the Degradation of AO10

Surfactants may be found in aqueous streams in numerous forms, including anionic, cationic and non-ionic surfactants, thereby complicating wastewater treatment. Anionic surfactants, such as carboxyl and sulfurate, have negatively charged hydrophilic groups. Surfactants derived from quaternary ammonium or phosphonium have hydrophilic groups that are positively charged. On the contrary, non-ionic surfactants, such as polymerized ethylene oxide, include a hydrophilic group that has been unionized. In a series of tests, the effect of different amounts of cationic and non-ionic surfactants (Triton X100, hexadecyl trimethyl ammonium bromide (CTAB) and Tween 80, respectively) on the UV/IO$_4^-$ oxidation process was determined. Figure 11 illustrates the yield of the dye breakdown with different surfactant concentrations.

Figure 11 demonstrates that the surfactant slows the breakdown of AO10, with comparable findings for Triton X100 and Tween 80. Tween 80 significantly affects the degradation process and limits the dye's degradation to 64.66%. After 40 min of reactions in the presence of surfactant, the degradation efficiency of AO10 was 90.00, 78.03, 77.13, 70.90, 68.61 and 64.66%, depending on the Tween 80 concentration: 0, 5, 20, 40, 60 and 80 mg/L. The degradation efficiency decreased from 91.00 to 69.42% when the Triton X100 concentration increased from 0 to 80 mg/L. This finding is consistent with Tween 20's impact on cinnamic acid degradation, as reported in a work available in the literature [46]. They show that cinnamic acid is distributed inside the micelle of the surfactant, protecting it against deterioration. In addition, they reported that the degradation process is much more pronounced at potentially higher acidic concentrations, even in micelle [46].

Figure 11. Effect of surfactants on the AO10 degradation ($[AO10]_0$ = 50 mg/L, 20 $\pm$ 1 °C, $[IO_4^-]$ = 3 mM, irradiation intensity: 15 mW/cm^2).

In general, more significant quantities of surfactants result in inadequate dye breakdown. This occurs because of "dye-surfactant interactions," which may result in (a) adsorption of dye on the micelle surface, (b) inclusion of dye in the palisade layer of the micelle, or (c) encapsulation of dye inside the micelle core. All these scenarios may alter the degradation of a dye. Surfactants have shown an inhibitory effect on the degradation of various contaminants by •OH-based AOPs [23,47–50].

In contrast to prior experimental observations generated from Triton X100 and Tween 80, CTAB (a cationic surfactant) runs indicate that a partial loss of AO10 degradation efficiency occurs only at a surfactant concentration of 5 mg/L. Moreover, the removal of the dye pollution was facilitated by increased CTAB concentrations. Using CTAB to remove ketoprofen, ibuprofen and diclofenac from wastewater, Liu et al. [51], got comparable results. Without a surfactant, the removal efficiency of ibuprofen, diclofenac and ketoprofen by the ECF method was reduced (44, 14 and 10%, respectively), while the addition of surfactant greatly enhanced the removal capacity of diclofenac, ibuprofen and ketoprofen from 12 to 97%, 12 to 88% and 6 to 82%, respectively.

3.8. Effect of Sucrose Addition

The UV/IO$_4^-$ treatment of AO10 solutions was also investigated in the presence of organic competitors, such as sucrose (water solubility= 2.1 10^3 g L^{-1}, K_{ow} = 2 10^{-4}, Henry's law constant= 4.4 10^{-22} atm m^3 mol^{-1}). Figure 12 depicts sucrose's (0.1–5 g L^{-1}) effect in the aqueous degradation of AO10 (5 g L^{-1}). The addition of sucrose partially inhibited the degradation of AO10, the effect being more marked at higher sucrose levels. After about 40 min process time, the AO10 degradation efficiency in the absence of sucrose was almost 91%, while it was about three times smaller at the highest test sucrose level.
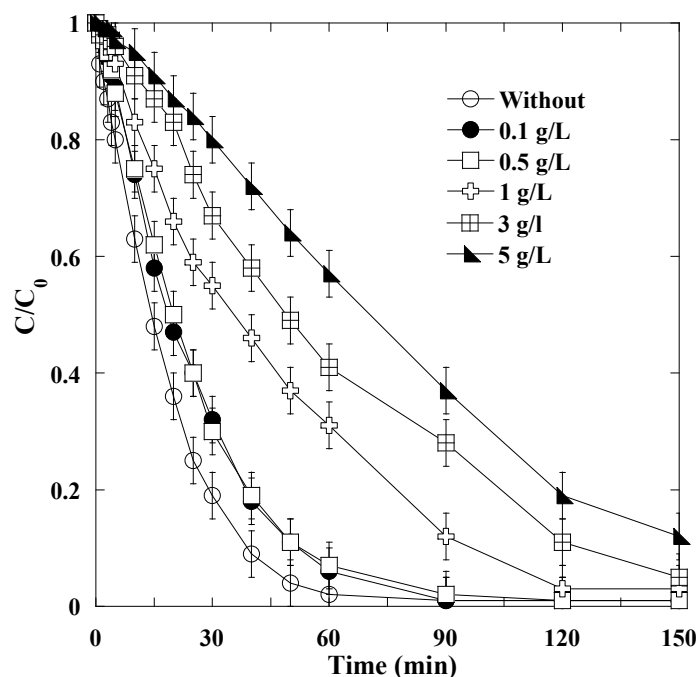
Figure 12. Sucrose's effect AO10 degradation ($[AO10]_0$ = 50 mg/L, 20 $\pm$ 1 °C, $[IO_4^-]$ = 3 mM, irradiation intensity: 15 mW/cm^2).

Morelli et al. [52] studied whether simple carbohydrates scavenged $^\bullet$OH radicals produced by the Fenton reaction; they found that disaccharides like maltose and sucrose were more successful than monosaccharides in eliminating $^\bullet$OH radicals. This finding supports the theory that the decrease in the efficiency of the Fenton process for the removal of AO10 in the presence of sucrose is attributable to a reduction in the quantity of accessible $^\bullet$OH radicals.
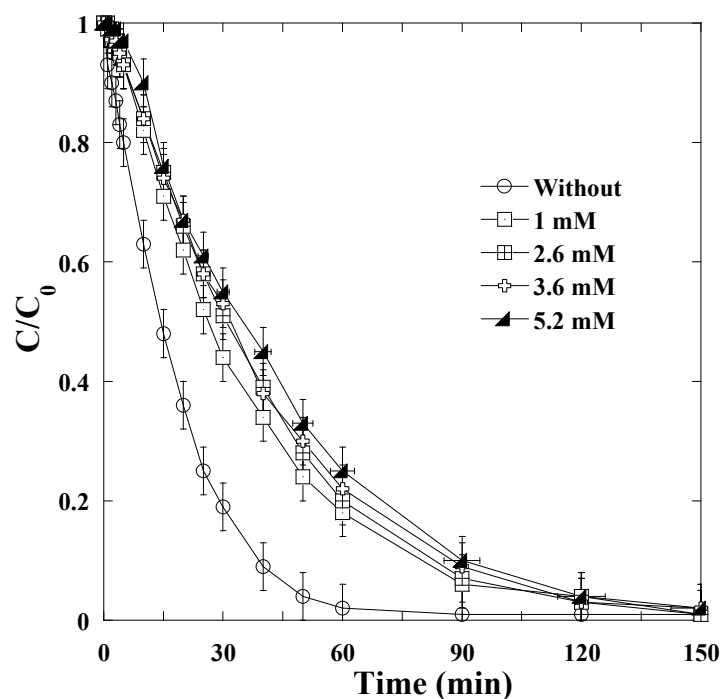
3.9. Effect of Tert-Butanol Addition

Photolysis of IO_4^- generates reactive species such as $O(^3P)$, $^\bullet$OH, $IO_3^\bullet$ and $IO_4^\bullet$, as discussed before. In this work, tert-butanol was utilized as a specific scavenger of hydroxyl radical (OH) and $O(^3P)$ during degradation of AO10 in the UV/IO_4^- system [23]. It is shown in Figure 13 how different concentrations of the alcohol tert-butanol (at 1, 2, 6, 8, and 10 mg L^{-1}) affect the degradation of 50 mg/L AO10. The degradation rate of AO10 slightly falls when tert-butanol is present, which indicates that both $^\bullet$OH and $O(^3P)$ play a limited part in the degradation of the dye and that the degradation process of AO10 in the UV/IO_4^- system is not dominated by a $^\bullet$OH and $O(^3P)$ pathway. $IO_3^\bullet$ and $IO_4^\bullet$ are much more critical in degrading dye than $^\bullet$OH and $O(^3P)$. A similar statement has been developed by Chia et al. [20] for the degradation of 4-chlorophenol.

3.10. Evolution of the Spectrum of the Reaction Mixture

Figure 14 shows the dye solution's UV–Visible spectrum fluctuations as a function of reaction time, which was used to investigate the changes in molecular and structural characteristics of AO10. A decrease in the absorbance at 477 nm, i.e., the dye's characteristic wavelength, occurs as the radiation time goes up. The aromatic and naphthenic derivatives of the dye absorb at around 254 and 330 nm; the peaks are abated rapidly during the treatment by the photoactivated periodate, as shown clearly in Figure 14. This result reflects the effective degradation of the aromatic rings in the dye molecules; the statement, which is confirmed by COD analysis, is reported in Figure 15. The COD removal efficiency was 56.46 and 60.50%, after process times of 60 and 120 min, respectively, thus demonstrating that the photoactivated periodate method did not wholly remove COD. It should be noted that after 120 min of treatment, the solution pH drops from 5.4 (initial value) to 3.6, reflecting

the formation of aliphatic acids (small chain) as final degradation products of AO10. However, these species could not be identified due to a lack of required instrumentation. For advancing the COD removal, post-injection of periodate could be proceeded to accelerate the destruction of the dye's degradation byproducts.

Figure 13. Effect of the addition of the tertbutanol on AO10 degradation ([AO10]$_0$ = 50 mg/L, 20 ± 1 °C, [IO$_4^-$] = 3 mM, irradiation intensity: 15 mW/cm^2).
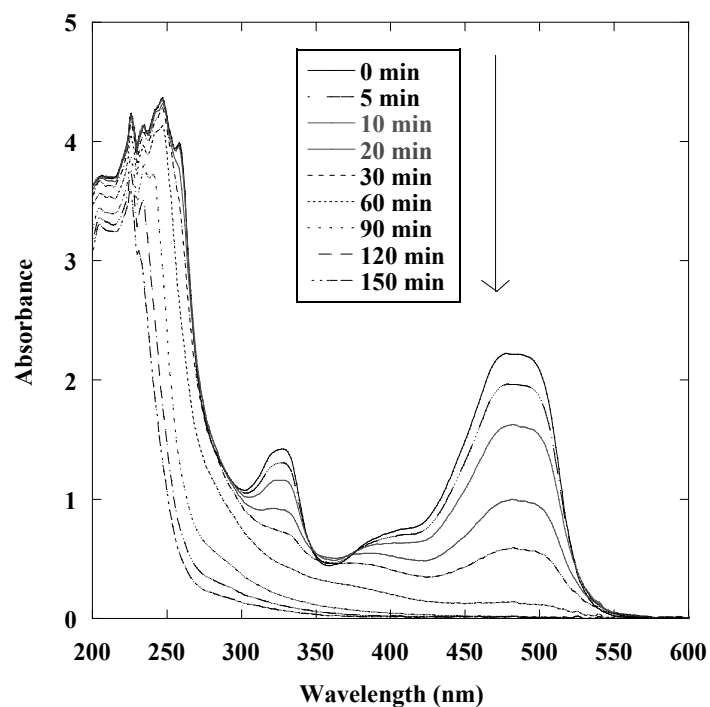
Figure 14. AO10 degradation UV–Visible absorption spectra ([AO10]$_0$ = 50 mg/L, 20 ± 1 °C, [IO$_4^-$] = 3 mM, irradiation intensity: 15 mW/cm^2).
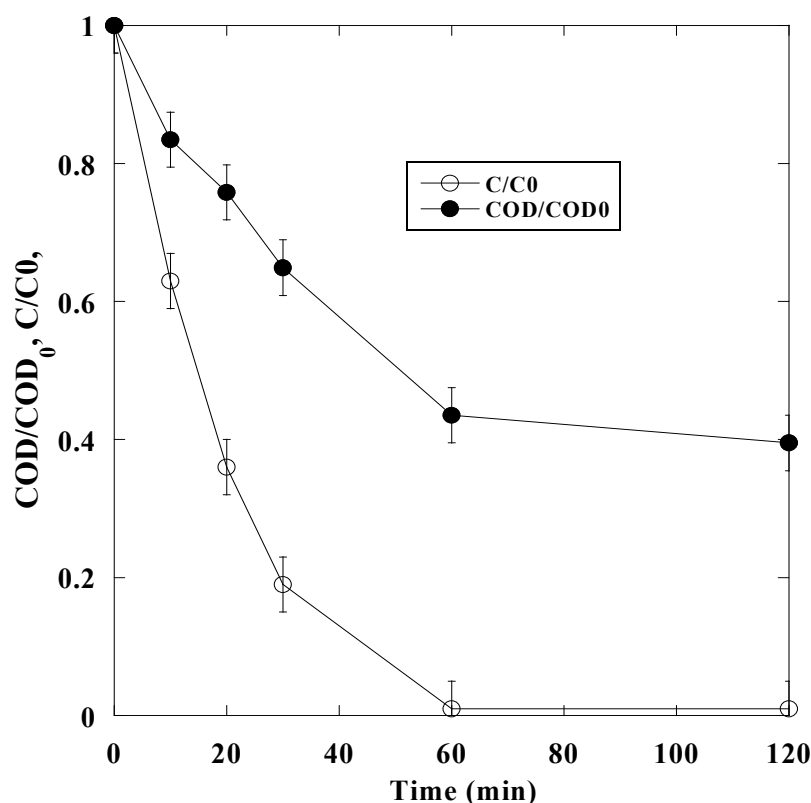
Figure 15. Removal of AO10 and measuring COD levels using the photoactivated periodate ($[AO10]_0$ = 50 mg/L, 20 ± 1 °C, $[IO_4^-]$ = 3 mM, irradiation intensity: 15 mW/cm^2).

4. Conclusions

The combination of UV and IO_4^- in aqueous solutions improved the breakdown of AO10 as compared to the sole UV photolysis. The initial degradation rate was a result of the action of oxidizing radicals generated at pH 5.4, which led to a faster breakdown. While in an acidic environment, $IO_4^\bullet$, $^\bullet$OH and O(3P) removed AO10, $IO_3^\bullet$ principally stimulated the removal by $^\bullet$OH and IO_3 in an alkaline environment. The dye's degradation rate increased with periodate dosage increase up to 3 mM, but decreased for higher values. The degradation rate of AO10 increased as the dye concentration rose from 10 to 75 mg/L; however, the inverse trend was recorded for the removal efficiency. The fastest degradation was determined at pH 5.4 (control pH). Even at low concentrations, surfactants decreased the extent of the dye degradation, but the degradation process may still occur when surfactant concentrations are very high. When salts are added to the dye solutions, the degradation rate also reduced. For UV/IO_4^- induced AO10 degradation to be most efficient, water must be as deionized as possible. Tert-butanol, a well-known scavenger of hydroxyl radicals, showed no noticeable effect on dye degradation even at high doses, reflecting the non-OH pathway of the degradation of this pollutant.

Finally, from the COD measurement results, it was clear that there is a complete elimination of dye but not of all organic matter (mineralization). The remaining products of photodegradation may be analyzed in future projects aimed at quantifying their amount and evaluate their toxicity, thereby extending the evaluation of the process viability.

Author Contributions: M.N. and H.G.: conceptualization, interpretation of results, writing, and editing. H.F., S.M., M.A., Y.B., M.B. and A.E.: interpretation of results, writing, and editing. All authors have read and agreed to the published version of the manuscript.

Conflicts of Interest: The authors declare no conflict of interest.

References

1. Kumar, P.; Govindaraju, M.; Senthamilselvi, S.; Premkumar, K. Photocatalytic degradation of methyl orange dye using silver (Ag) nanoparticles synthesized from Ulva lactuca. *Colloids Surf. B Biointerfaces* **2013**, *103*, 658–661. [CrossRef] [PubMed]
2. Nezamzadeh-Ejhieh, A.; Khorsandi, M. Heterogeneous photodecolorization of Eriochrome Black T using Ni/P zeolite catalyst. *Desalination* **2010**, *262*, 79–85. [CrossRef]
3. Pearce, C.I.; Lloyd, J.R.; Guthrie, J.T. The removal of colour from textile wastewater using whole bacterial cells: A review. *Dyes Pigments* **2003**, *58*, 179–196. [CrossRef]
4. Nachiyar, C.V.; Rajkumar, G.S. Degradation of a tannery and textile dye, Navitan Fast Blue S5R by *Pseudomonas aeruginosa*. *World J. Microbiol. Biotechnol.* **2003**, *19*, 609–614. [CrossRef]
5. Kalyani, D.C.; Patil, P.S.; Jadhav, J.P.; Govindwar, S.P. Biodegradation of reactive textile dye Red BLI by an isolated bacterium *Pseudomonas* sp. SUK1. *Bioresour. Technol.* **2008**, *99*, 4635–4641. [CrossRef]
6. Aquino, J.M.; Rocha-Filho, R.C.; Ruotolo, L.A.M.; Bocchi, N.; Biaggio, S.R. Electrochemical degradation of a real textile wastewater using β-PbO_2 and DSA® anodes. *Chem. Eng. J.* **2014**, *251*, 138–145. [CrossRef]
7. Khatri, J.; Nidheesh, P.V.; Singh, T.S.A.; Kumar, M.S. Advanced oxidation processes based on zero-valent aluminium for treating textile wastewater. *Chem. Eng. J.* **2018**, *348*, 67–73. [CrossRef]
8. Kishor, R.; Purchase, D.; Saratale, G.D.; Saratale, R.G.; Ferreira, L.F.R.; Bilal, M.; Chandra, R.; Bharagava, R.N. Ecotoxicological and health concerns of persistent coloring pollutants of textile industry wastewater and treatment approaches for environmental safety. *J. Environ. Chem. Eng.* **2021**, *9*, 105012. [CrossRef]
9. Sukhatskiy, Y.; Shepida, M.; Sozanskyi, M.; Znak, Z.; Gogate, P.R. Periodate-based advanced oxidation processes for wastewater treatment: A review. *Sep. Purif. Technol.* **2023**, *304*, 122305. [CrossRef]
10. Chadi, N.E.; Merouani, S.; Hamdaoui, O.; Bouhelassa, M.; Ashokkumar, M. H_2O_2/Periodate (IO_4^-): A novel advanced oxidation technology for the degradation of refractory organic pollutants. *Environ. Sci. Water Res. Technol.* **2019**, *5*, 1113–1123. [CrossRef]
11. Li, X.; Liu, X.; Qi, C.; Lin, C. Activation of periodate by granular activated carbon for acid orange 7 decolorization. *J. Taiwan Inst. Chem. Eng.* **2016**, *68*, 211–217. [CrossRef]
12. Li, X.; Liu, X.; Lin, C.; Qi, C.; Zhang, H.; Ma, J. Enhanced activation of periodate by iodine-doped granular activated carbon for organic contaminant degradation. *Chemosphere* **2017**, *181*, 609–618. [CrossRef]
13. Peng, J.; Wang, Z.; Wang, S.; Liu, J.; Zhang, Y.; Wang, B.; Gong, Z.; Wang, M.; Dong, H.; Shi, J.; et al. Enhanced removal of methylparaben mediated by cobalt/carbon nanotubes (Co/CNTs) activated peroxymonosulfate in chloride-containing water: Reaction kinetics, mechanisms and pathways. *Chem. Eng. J.* **2021**, *409*, 128176. [CrossRef]
14. Saien, J.; Shafiei, H.; Amisama, A. Photo-activated periodate in homogeneous degradation and mineralization of Quinoline: Optimization, kinetic, and energy consumption. *Environ. Prog. Sustain. Energy* **2017**, *36*, 1621–1627. [CrossRef]
15. Barat, F.; Gilles, L.; Hickel, B.; Lesigne, B. Transient species in the pulse radiolysis of periodate ion in neutral aqueous solutions. *Chem. Commun.* **1971**, *847*, 847–848. [CrossRef]
16. Bhattacharyya, S.N.; Bardhan, D.K. Radiolysis of aqueous solution of potassium periodate. *Bull. Chem. Soc. Jpn.* **1970**, *43*, 2808–2811. [CrossRef]
17. Kläning, U.K.; Sehested, K.; Wolff, T. Laser flash photolysis and pulse radiolysis of iodate and periodate in aqueous solution. Properties of iodine (VI). *J. Chem. Soc. Faraday Trans. 1 Phys. Chem. Condens. Phases* **1981**, *77*, 1707–1718. [CrossRef]
18. Patil, S.F.; Patil, R.M.; Mudaliar, M. Effect of iso-propanol on the radiolysis of aqueous solutions of periodate. *J. Radioanal. Nucl. Chem.* **1990**, *139*, 323–329. [CrossRef]
19. Wagner, I.; Strehlow, H. Flash Photolysis in Aqueous Periodate-Solutions. *Ber. Bunsenges. Phys. Chem.* **1982**, *86*, 297–301. [CrossRef]
20. Chia, L.-H.; Tang, X.; Weavers, L.K. Kinetics and mechanism of photoactivated periodate reaction with 4-chlorophenol in acidic solution. *Environ. Sci. Technol.* **2004**, *38*, 6875–6880. [CrossRef]
21. Ghodbane, H.; Hamdaoui, O. Degradation of anthraquinonic dye in water by photoactivated periodate. *Desalin. Water Treat.* **2016**, *57*, 4100–4109. [CrossRef]

22. Hamdaoui, O.; Merouani, S. Improvement of sonochemical degradation of brilliant blue R in water using periodate ions: Implication of iodine radicals in the oxidation process. *Ultrason. Sonochem.* **2017**, *37*, 344–350. [CrossRef] [PubMed]

23. Bendjama, H.; Merouani, S.; Hamdaoui, O.; Bouhelassa, M. Efficient degradation method of emerging organic pollutants in marine environment using UV/periodate process: Case of chlorazol black. *Mar. Pollut. Bull.* **2018**, *126*, 557–564. [CrossRef] [PubMed]

24. Lee, C.; Yoon, J. Application of photoactivated periodate to the decolorization of reactive dye: Reaction parameters and mechanism. *J. Photochem. Photobiol. A Chem.* **2004**, *165*, 35–41. [CrossRef]

25. Tang, X.; Weavers, L.K. Using photoactivated periodate to decompose TOC from hydrolysates of chemical warfare agents. *J. Photochem. Photobiol. A Chem.* **2008**, *194*, 212–219. [CrossRef]

26. Tang, X.; Weavers, L.K. Decomposition of hydrolysates of chemical warfare agents using photoactivated periodate. *J. Photochem. Photobiol. A Chem.* **2007**, *187*, 311–318. [CrossRef]

27. Weavers, L.K.; Hua, I.; Hoffmann, M.R. Degradation of triethanolamine and chemical oxygen demand reduction in wastewater by photoactivated periodate. *Water Environ. Res.* **1997**, *69*, 1112–1119. [CrossRef]

28. Saien, J.; Fallah Vahed Bazkiaei, M. Homogenous UV/periodate process in treatment of p-nitrophenol aqueous solutions under mild operating conditions. *Environ. Technol.* **2018**, *39*, 1823–1832. [CrossRef]

29. Zhang, X.; Yu, X.; Yu, X.; Kamali, M.; Appels, L.; Van der Bruggen, B.; Cabooter, D.; Dewil, R. Efficiency and mechanism of 2, 4-dichlorophenol degradation by the UV/IO4−process. *Sci. Total Environ.* **2021**, *782*, 146781. [CrossRef]

30. Tian, F.-X.; Hu, X.-J.; Xu, B.; Zhang, T.-Y.; Gao, Y.-Q. Phototransformation of iodate by UV irradiation: Kinetics and iodinated trihalomethane formation during subsequent chlor (am) ination. *J. Hazard. Mater.* **2017**, *326*, 138–144. [CrossRef]

31. Filip, J.; Cajthaml, T.; Najmanová, P.; Černík, M.; Zbořil, R. *Advanced Nano-Bio Technologies for Water and Soil Treatment*; Springer Nature: Cham, Switzerland, 2020; ISBN 3030298396.

32. Ilin, A.; Nersesyan, A. Toxicology of iodine: A mini review. *Arch. Oncol.* **2013**, *21*, 65–71. [CrossRef]

33. Thomas, O.; Mazas, N. La mesure de la demande chimique en oxygène dans les milieux faiblement pollués. *Analusis* **1986**, *14*, 300–302.

34. Bendjama, H.; Merouani, S.; Hamdaoui, O.; Bouhelassa, M. Using photoactivated acetone for the degradation of Chlorazol Black in aqueous solutions: Impact of mineral and organic additives. *Sci. Total Environ.* **2019**, *653*, 833–838. [CrossRef] [PubMed]

35. Barat, F.; Gilles, L.; Hickel, B.; Lesigne, B. Pulsed radiolysis and flash photolysis of iodates in aqueous solution. *J. Phys. Chem.* **1972**, *76*, 302–307. [CrossRef]

36. Bokare, A.D.; Choi, W. Singlet-Oxygen generation in alkaline periodate solution. *Environ. Sci. Technol.* **2015**, *49*, 14392–14400. [CrossRef] [PubMed]

37. Klaning, U.K.; Sehested, K. Photolysis of periodate and periodic acid in aqueous solution. *J. Chem. Soc. Faraday Trans. 1 Phys. Chem. Condens. Phases* **1978**, *74*, 2818–2838. [CrossRef]

38. Bendjama, H.; Merouani, S.; Hamdaoui, O.; Bouhelassa, M. Acetone photoactivated process: Application to the degradation of refractory organic pollutants in very saline waters. *Water Environ. J.* **2019**, *34*, 1–8. [CrossRef]

39. Hamdaoui, O.; Merouani, S. Ultrasonic destruction of acid Orange 7: Effect of humic acid, surfactants and complex matrices. *Water Environ. Res.* **2017**, *89*, 250–259. [CrossRef]

40. Belghit, A.A.; Merouani, S.; Hamdaoui, O.; Bouhelassa, M.; Alghyamah, A.; Bouhelassa, M. Influence of processing conditions on the synergism between UV irradiation and chlorine toward the degradation of refractory organic pollutants in UV/chlorine advanced oxidation system. *Sci. Total Environ.* **2020**, *736*, 139623. [CrossRef]

41. Chadi, N.E.; Merouani, S.; Hamdaoui, O.; Bouhelassa, M.; Ashokkumar, M. Influence of mineral water constituents, organic matter and water matrices on the performance of the H_2O_2/IO_4^--Advanced oxidation process. *Environ. Sci. Water Res. Technol.* **2019**, *5*, 1985–1992. [CrossRef]

42. Stefan, M.I. *Advanced Oxidation Processes for Water Treatment: Fundamentals and Applications*; IWA Publishing: London, UK, 2017.

43. Gu, X.; Lu, S.; Li, L.; Qiu, Z.; Sui, Q.; Lin, K.; Luo, Q. Oxidation of 1, 1, 1-Trichloroethane Stimulated by Thermally Activated Persulfate. *Ind. Eng. Chem. Res.* **2011**, *50*, 11029–11036. [CrossRef]

44. Wang, Z.; Yuan, R.; Guo, Y.; Xu, L.; Liu, J. Effects of chloride ions on bleaching of azo dyes by Co^{2+}/oxone regent: Kinetic analysis. *J. Hazard. Mater.* **2011**, *190*, 1083–1087. [CrossRef] [PubMed]

45. Yang, S.; Wang, P.; Yang, X.; Shan, L.; Zhang, W.; Shao, X.; Niu, R. Degradation efficiencies of azo dye Acid Orange 7 by the interaction of heat, UV and anions with common oxidants: Persulfate, peroxymonosulfate and hydrogen peroxide. *J. Hazard. Mater.* **2010**, *179*, 552–558. [CrossRef] [PubMed]

46. Ugazio, E.; Carlotti, M.E.; Sapino, S.; Trotta, M.; Vione, D.; Minero, C. Photodegradation of cinnamic acid in different media. *J. Dispers. Sci. Technol.* **2008**, *29*, 641–652. [CrossRef]

47. Bekkouche, S.; Merouani, S.; Hamdaoui, O.; Bouhelassa, M. Efficient photocatalytic degradation of Safranin O by integrating solar-UV/TiO2/persulfate treatment: Implication of sulfate radical in the oxidation process and effect of various water matrix components. *J. Photochem. Photobiol. A Chem.* **2017**, *345*, 80–91. [CrossRef]

48. Almarhabi, S.; Ashokkumar, M. Sonochemical degradation of p-toluenesulfonic acid in aqueous environment. *Energy Environ. Focus* **2015**, *4*, 239–244. [CrossRef]

49. Destaillats, H.; Alderson, T.W.; Hoffmann, M.R. Applications of ultrasound in NAPL remediation: Sonochemical degradation of TCE in aqueous surfactant solutions. *Environ. Sci. Technol.* **2001**, *35*, 3019–3024. [CrossRef]

50. Rayaroth, M.P.; Aravind, U.K.; Aravindakumar, C.T. Sonochemical degradation of Coomassie Brilliant Blue: Effect of frequency, power density, pH and various additives. *Chemosphere* **2015**, *119*, 848–855. [CrossRef]
51. Liu, Y.-J.; Lo, S.-L.; Liou, Y.-H.; Hu, C.-Y. Removal of nonsteroidal anti-inflammatory drugs (NSAIDs) by electrocoagulation–flotation with a cationic surfactant. *Sep. Purif. Technol.* **2015**, *152*, 148–154. [CrossRef]
52. Morelli, R.; Russo-Volpe, S.; Bruno, N.; Lo Scalzo, R. Fenton-dependent damage to carbohydrates: Free radical scavenging activity of some simple sugars. *J. Agric. Food Chem.* **2003**, *51*, 7418–7425. [CrossRef]